Temperature dependence of the photoluminescence of all-porous-silicon optical microcavities

M. Cazzanelli,[a] C. Vinegoni, and L. Pavesi[b]
Istituto Nazionale di Fisica della Materia and Dipartimento di Fisica, Università di Trento, Via Sommarive 14, I-38050 Povo (TN), Italy

(Received 29 July 1998; accepted for publication 27 October 1998)

Photoluminescence measurements in all-porous-silicon optical microcavities (PSM) are reported over a wide temperature range. Both continuous wave and time resolved measurements have been performed. The microcavity is formed by an all porous silicon Fabry–Perot filter made by two distributed Bragg reflectors separated by a λ-thick PS cavity layer. The luminescence properties of PSM are changed with respect to those of PS: a temperature independent narrowing in the emission line shape, a different temperature dependence of the emission intensity, and a fractional shortening of the luminescence decay time over the 50–300 K temperature interval are achieved. The PSM luminescence properties are explained by the spatial redistribution of the spontaneous emission, by an effective refractive index probed by the photon mode confined in the cavity layer and by the coupling between the singlet exciton state and the photon mode confined in the cavity layer. The saturation of the absorption of the distributed Bragg reflector is also addressed. © *1999 American Institute of Physics.* [S0021-8979(99)04503-X]

I. INTRODUCTION

The emission properties of silicon, an indirect band-gap semiconductor, are much improved in porous silicon (PS) by electron confinement.[1] After a partial anodic dissolution of silicon wafers, Si nanocrystals arranged spatially in a highly constrained and filamentary geometry are produced in PS. Electron confinement in these Si nanocrystals yields an enlargement of the band gap and an efficient emission in the visible at room temperature. If one couples the electron confinement with the photon confinement,[2] the emission properties of silicon are further changed: a narrowing, an increase in the emission efficiency, a fractional shortening of the lifetime, and a strong directionality of the emission pattern are all observed.[3]

Two dimensional photon confinement in PS can be obtained by the use of a Fabry–Perot structure formed with PS multilayers.[4] Porosity multilayers can be grown by modulating the current density during the silicon etching in such a way that both the refractive index and the thickness of each layer are changed. Owing to the great control reached in the PS multilayers formation, it is possible to grow λ/4 stacks and with them Fabry–Perot structure with a high finesse. A dielectric Fabry–Perot filter is formed by an optical cavity made by two dielectric Bragg reflectors (mirrors) separated by a λ-thick PS layer (cavity). A review on PS microcavities (PSM) is reported in Ref. 3.

The room temperature photoluminescence (PL) properties of PSM have been studied in Ref. 4, while a thorough discussion of the time decay of the PSM luminescence has been presented in Ref. 5. The main conclusions are here summarized. The modified luminescence line shape in PSM is caused by the redistribution of the PS emission in space and by its concentration into the cavity photon mode. The variations in the emission lifetime are due to the change of the local dielectric environment caused by the finite penetration depth of the cavity photon mode into the mirrors. In fact, the spontaneous emission rate $R_{sp}(\hbar\omega)$ for a bulk material is given by

$$R_{sp}(\hbar\omega) \propto M(\hbar\omega) \times G(\hbar\omega), \tag{1}$$

where, for simplicity, the electronic, $M(\hbar\omega)$, and the photonic, $G(\hbar\omega)$, contributions have been separated. The photon mode density $G(\hbar\omega)$ is

$$G(\hbar\omega) = \frac{n^3(\hbar\omega)^2}{\pi^2 c^3 \hbar^3}, \tag{2}$$

where n is a refractive index. In PSM, only $G(\hbar\omega)$ is varied while $M(\hbar\omega)$ is the same as that of PS because the cavity material is PS itself. In general, the electronic transitions couple to the optical modes which have an energy $\hbar\omega$ equal to the transition energy. In a microcavity the electronic transition occurs in the cavity layer, however the photon cavity mode, to which the excitonic transition couples, is extending also into the mirrors. Consequently, the refractive index entering into Eq. (2) is a thickness-weighted average of the refractive indexes of the layers where the photon cavity mode extends. Hence, the luminescence time decays are different in PSM and in PS due to the different n values.

However some questions still remain: (i) why the dielectric effect is observed at room temperature where the lifetime is essentially dominated by non radiative effects; (ii) as the mirrors are made by PS and, thus, they luminesce, what is the balance between the mirrors and the cavity emissions; (iii) is the linewidth of the emission determined by the cavity

[a]Present address: Group of Applied Physics, University of Geneve, Rue de L'Ecole de Medecine, CH-1211 Geneva 4, Switzerland.
[b]To whom correspondence should be addressed; electronic mail: pavesi@science.unitn.it

finesse or do other effects play a role, (iv) what is the role of the exciton-photon coupling in PSM. The present article reports on a study of the luminescence of PSM as a function of temperature and excitation intensity aiming to address these questions.

II. EXPERIMENTAL DETAILS

The PSM used in this work are detailed in Refs. 6 and 4. Mainly two samples have been investigated: sample A has a record linewidth of 2 nm and it is representative of the samples produced as in Ref. 6; while sample B has a linewidth of 15 nm and represents more standard samples. The growth procedure and other experimental details are lengthly reviewed in Ref. 3. Here it suffices to say that the samples have been grown on 0.01 Ω cm *p*-type doped substrates by using a computer-controlled standard electrochemical setup. Sample A has the following characteristics:[6] the mirrors are formed by two random Bragg reflectors with 10 periods of a low refractive index ($n=1.5$) layer of 60% porosity (randomly distributed with a mean thickness=133 nm) and of a high refractive index ($n=2.24$) layer of 43% porosity (89 nm thick). The mirrors have a symmetric distribution of the random layer thicknesses around the cavity layer. This last one has a thickness of 623 nm and is obtained by using a porosity of 75% ($n=1.27$). Sample B is characterized by a λ thick cavity layer of 75% porosity ($n=1.27$, 598 nm thick) with the mirrors formed by Bragg reflectors composed of 6 pairs of alternating λ/4 layer with porosities of 62% ($n=1.50$, 126 nm thick) and 45% ($n=2.24$, 84 nm thick), respectively.

The time resolved measurements have been performed by using a frequency doubled Ti:sapphire laser. A pulse-picker stage allowed to change the frequency repetition of the laser so that the lengthening of the PL decay of PS as the temperature decreases can be followed. Care was taken to use the same pulse power independently of the frequency repetition. The continuous wave (cw) luminescence measurements have been performed with the 488 nm line of an air-cooled Ar laser. The samples were placed in a continuous flow cryostat whose temperature can be changed continuously from 6 up to 300 K. A true backscattering configuration has been used to collect the luminescence.

III. DATA

A. Temperature dependence

In Fig. 1 the PL spectra of sample A have been reported for various temperatures, *T*. The use of a microcavity sample is clearly observed in the line shape of the emission spectrum. The wide emission band of PS is replaced by a single peaked emission spectrum centered at λ_c, the cavity wavelength. The luminescence at the peak position comes from the recombination in the cavity layer. On the contrary to what happens for III–V semiconductor based microcavities, in PSM the mirror material is the same as the cavity material (i.e., the same band gap and the same spectral emission position). As a consequence, the emission for $\lambda \neq \lambda_c$ is due to the recombination which occurs in the mirror spatial region.

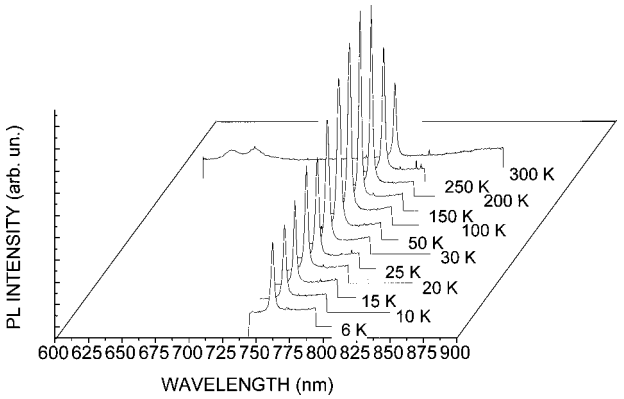

FIG. 1. Photoluminescence as a function of temperature for sample A. The spectra have been shifted for clarity. The horizontal line is the baseline for each spectrum. The measurement temperatures are given on the right.

As *T* increases, the line shape is unchanged, the main variation is in the relative emission intensity from the cavity and the mirrors. In the figure, the various PL spectra are all normalized to the mirror emission. Thus one observes an increased emission from the cavity for *T* up to 150 K, then for higher *T* the emission of the cavity weakens with respect to the mirror emission. Other details of the temperature dependence of the emissions are reported in Fig. 2.

Figure 2(a) shows the peak intensity (I_{PL}) of the cavity resonance mode as a function of *T*. A bell-shaped curve is measured as with standard PS samples.[1] This behavior has been explained as due to the interplay of radiative and nonradiative recombinations. At low *T* the PL is dominated by

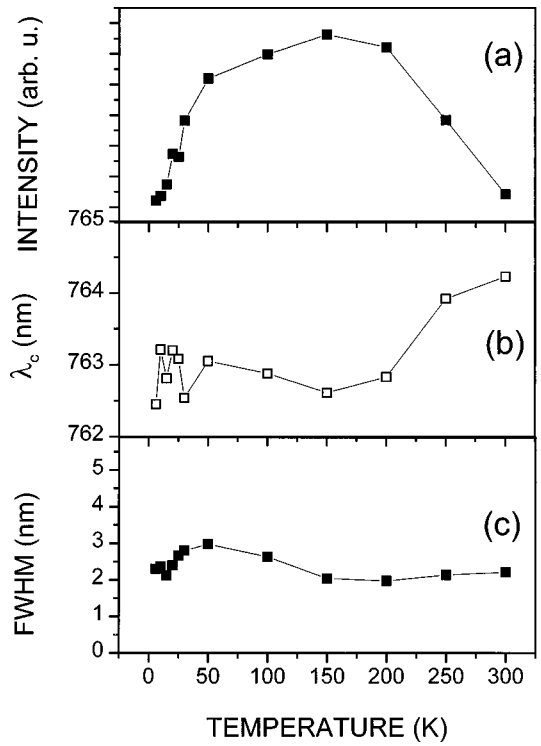

FIG. 2. Summary of the temperature dependence of some parameters extracted from the luminescence of sample A. The top panel reports the peak intensity of the cavity mode, the central panel the spectral position, and the bottom panel the full width at half maximum (FWHM).

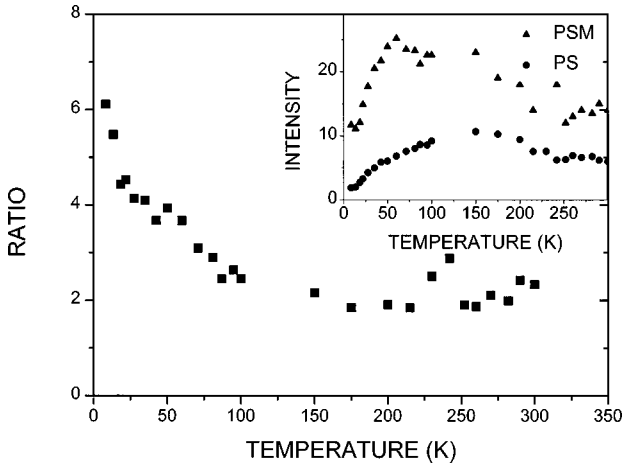

FIG. 3. Comparison of the photoluminescence intensity ratio of a PSM (sample B) and of a reference PS sample as a function of the temperature, at the cavity emission wavelength. The inset shows the bare data for the reference PS sample (circles) and the PSM (triangles).

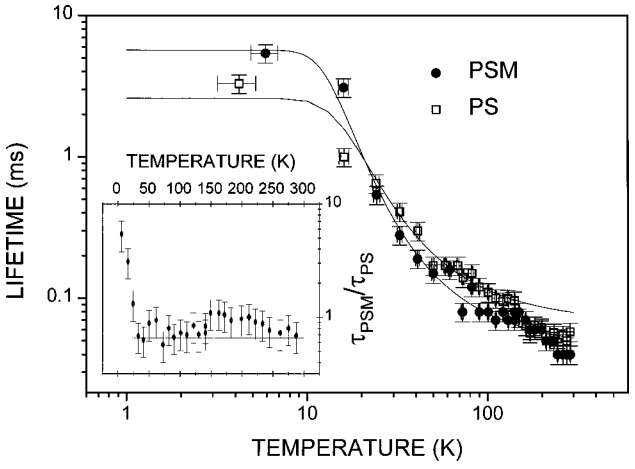

FIG. 4. Temperature dependence of the luminescence decay time at the wavelength of the cavity mode (λ_c) for the PS (empty squares) and the PSM sample (filled circles) as deduced by a stretched exponential fit of the experimental decays. The lines are fits with Eq. (4) which yield the parameters reported in Table I. The inset shows the ratio between the lifetimes of PSM (τ_{PSM}) and of PS (τ_{PS}). The horizontal line indicates the 2/3 value which is the value theoretically expected for ideal microcavities.

radiative recombinations, where the radiative lifetime is due to the thermal balance between occupation of the dipole-prohibited triplet state and the dipole-allowed high energy singlet state (see more later). As T increases the singlet population increases in turn and the luminescence intensity increases. When T is high enough, fast nonradiative recombinations occur and the luminescence intensity decreases. This general trend is respected in Fig. 2(a).

Figure 2(b) reports the T dependence of the cavity peak position. As T is decreased from room temperature down to 150 K, λ_c decreases. Further decreasing T, λ_c stays constant within the experimental errors. The decreases in λ_c reflects the temperature variation of the refractive index n: $\lambda_c = n \times d$, where d is the cavity thickness. The full width at half maximum of the emission peak ($\Delta\lambda$) is given in Fig. 2(c). The nearly independence of $\Delta\lambda$ on T indicates that the linewidth of the cavity mode is determined solely by the microcavity structure and not by the excitonic thermalization in all the T range here investigated.

It is of interest to know how the enhancement of the emission intensity (I_{PL}) observed for PSM depends on T. This is reported in Fig. 3, where the ratio (γ) of I_{PL} at λ_c for sample B and for the reference PS sample is shown as a function of T. We note that the absolute value of γ is sample and age dependent and values as high as 20 can be obtained.[3] A detailed study of these aspects are referred to a forthcoming article. Here we want to address only the trend. For this sample $\gamma \simeq 2$ at room temperature. γ is almost independent on T as long as $T > 100$ K, while it increases strongly with T at low T. The inset shows the T dependence of I_{PL} at λ_c for the PSM and the reference PS sample. A bell-shaped I_{PL} profile is measured for both samples but the I_{PL} maximum occurs at lower T for PSM than for PS.

To further investigate this aspect, time resolved measurements have been performed. It is well known that in PS the luminescence decay is fitted by a stretched exponential function due to the complicated diffusion dynamics of the excited excitons in this disordered system.[7] The stretched exponential function is

$$I(t) = I_0 \exp(-t/\tau)^{\beta}, \tag{3}$$

where τ and β are the average lifetime and the dispersion exponent, respectively. By using Eq. (3) we have extracted from the experimental data τ and β. The T dependence of τ is reported in Fig. 4 for PSM and PS at λ_c. The same trend as that observed for usual PS samples is observed.[7] As what concerns β (not shown in the figure), it is constant from 300 down to 100 K, and then decreases as T is decreased. Both these trends have been already explained: for τ by introducing a two levels system (singlet and triplet excitons) and by assuming the exciton thermalization between them,[8] for β by assuming a dispersive diffusion of excitons in a disordered Si-nanocrystals arrangement and by introducing the trap-controlled hopping of excitons.[7]

The τ vs T dependence can be described by the temperature dependence of the occupation of the singlet and triplet levels:[8]

$$\tau_{rad}(T) = \tau_{trip}\left[\frac{1 + (1/3)\exp(-\Delta E_x/k_B T)}{1 + (1/3)(\tau_{trip}/\tau_{sing})\exp(-\Delta E_x/k_B T)}\right], \tag{4}$$

where τ_{trip} is the triplet lifetime, τ_{sing} the singlet lifetime, and ΔE_x the singlet-triplet energy splitting. A fit of the experimental data for $T < 150$ K (see Fig. 4) yields the parameters reported in the Table I. ΔE_x is essentially unchanged by the cavity structure while the singlet and triplet lifetimes show different values in PSM and PS. In the last column of the table, the data for $\lambda \neq \lambda_c$, i.e., representative of the mirror emission, are reported. As already noted in Ref. 5 the mirror luminescence decays faster than the cavity luminescence due to a larger effective refractive index, cf. Eq. (2).

The inset of Fig. 4 shows the ratio of the PSM and PS lifetime at λ_c. This is lower than one (i.e., the lifetime of PSM is shorter than that of PS within the error bars) down to 40 K where it grows. This is the temperature region where the recombination from triplet states predominates.

TABLE I. Results of the least square fitting of the temperature dependence of the luminescence lifetimes shown in Fig. 4 with Eq. (4). ΔE_x, τ_{trip}, and τ_{sing} are the triplet-singlet splitting energy, the triplet lifetime, and the singlet lifetime, respectively.

Sample	ΔE_x (meV)	τ_{trip} (ms)	τ_{sing} (μs)
PS (at λ_c)	6±0.4	2.6±0.7	17±1
PSM (at λ_c)	7±0.3	5.9±0.6	10±1
PSM (at $\lambda = 695$ nm)	7±0.6	1±0.2	8±1

B. Excitation intensity dependence

The variations of the PL spectra at room temperature for sample A and for various excitation intensities (J_{exc}) are reported in Fig. 5. As J_{exc} increases, the cavity mode emerges from the background of the mirror luminescence and a well resolved peak is measured.

The J_{exc} dependence of I_{PL} is shown in Fig. 6 for sample B and for various T. $I_{PL} \propto J_{exc}^{\alpha}$ with $\alpha \leqslant 1$. α vs T is shown in Fig. 7. An almost constant α is found. Only at low T, α decreases to roughly 0.5. On the other hand, τ and β are roughly constant when J_{exc} is varied.

IV. DISCUSSION

The present experimental data support the conclusions reached in Ref. 5 which are based on the theoretical work of Ref. 2. In addition, the following points can be stated:

(1) The effect of the microcavity is to change significantly the singlet lifetime. This is a result of the fact that the singlet state is dipole allowed, and hence can couple with the photons, while the triplet state being dipole prohibited, cannot couple with. The variations in τ_{tripl} observed in Table I are more likely sample dependent and are not influenced by the microcavity structure.

(2) The coupling of the singlet state with the photon mode reduces the singlet lifetime in the PSM. This contributes to the increase in the overall luminescence intensity and to the fractional shortening of the time decay of the luminescence (which is also dependent on the local dielectric environment).

(3) The luminescence lifetime at low temperature (here identified with τ_{tripl}) is due to the balance between the nonradiative and the radiative, but not dipole allowed, recombinations (see Fig. 2 in Ref. 7). The results for the different samples are due to sample dependent properties rather than to the microcavity structures.

(4) It is mainly in the intermediate temperature range where the thermal population of the singlet state is important that the two levels internal structure of the excitons in PS plays a role. The different T of the maxima of I_{PL} for PSM and PS are explained by the lower τ_{sing} in PSM than in PS. In PSM samples with a very long τ_{tripl} as those reported in Ref. 4, I_{PL} increases monotonously even at low T. At room T, the lifetime is again due to the balance of radiative and nonradiative recombinations. However, as already observed in Ref. 9:

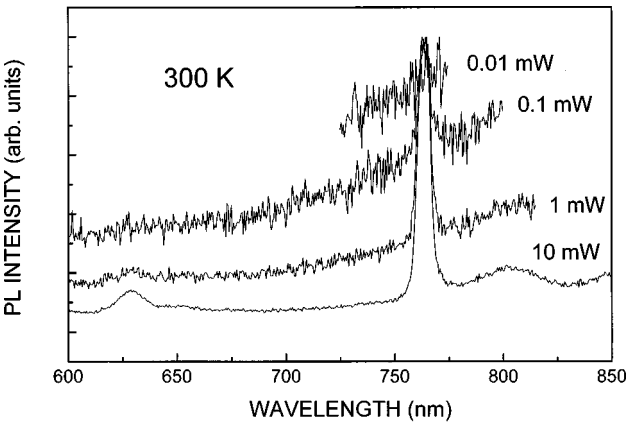

FIG. 5. Incident intensity dependence of the luminescence spectrum of sample B. The various spectra have been normalized to their maximum. The temperature was 300 K. The excitation area was 3×10^{-4} cm^2.

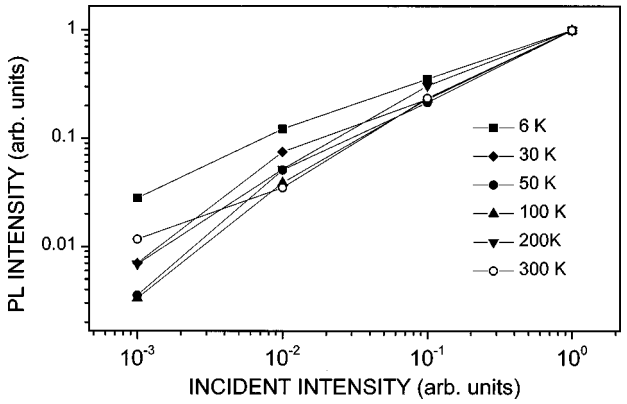

FIG. 6. Incident intensity dependence of the photoluminescence peak intensity at the cavity mode for the various temperatures indicated on the figure. The intensity has been normalized to the maximum intensity used.

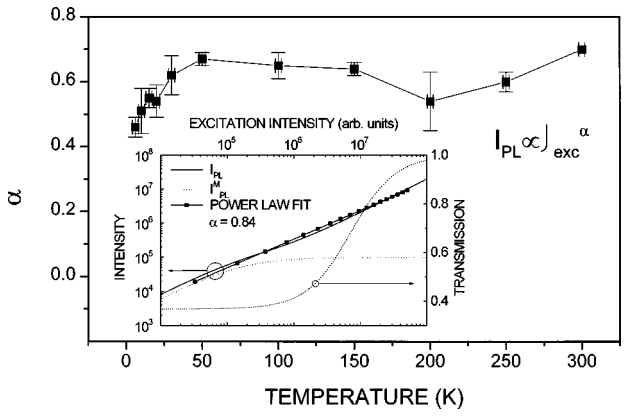

FIG. 7. Temperature dependence of the α exponent defined as the formula given in the figure, where I_{PL} is the peak intensity at the cavity wavelength and J_{exc} the excitation intensity. The PSM sample B has been used. The inset shows the result of the simple model described in Sec. IV. The dashed line is the transmission coefficient T, the dotted line the luminescence from the mirror [I_{PL}^{M}, see Eq. (7)] and the full line the total luminescence intensity [I_{PL}, see Eq. (6)]. The squares refer to the result of a power law fit with $\alpha = 0.84$.

$$W_{\mathrm{tot}}(n)=W_{\mathrm{nr}}+W_r\simeq W_{\mathrm{nr}}+f(n)W_r^0, \tag{5}$$

where W_{xxx} are the total ($xxx=\mathrm{tot}$), nonradiative ($xxx=\mathrm{nr}$), and radiative ($xxx=r$) recombination rates, respectively. W_r^0 is the PS radiative recombination rate in absence of the microcavity structure. $f(n)$ is a function which explicates the dependence of the radiative recombination rate on the effective refractive index, already introduced in Eq. (2) and discussed in Ref. 5. W_{nr} is independent on n. Equation (5) explains why the microcavity effects, i.e., the variation of W_r with n through $f(n)$, are observed even at room temperature where W_{nr} is large.

(5) The J_{exc} dependence of the PL spectra shown in Fig. 5 is due to the saturation of the mirror absorption as the excitation intensity is increased. As more excitons are directly photogenerated in the cavity layer due to the increased transparency of the mirror (result of the absorption saturation), the luminescence at the cavity wavelength increases with respect to that at the other wavelength.

(6) The power dependence of the PL intensity at λ_c and the temperature dependence of the α exponent are due to the saturation of the mirror emission at λ_c. In fact, the luminescence at λ_c is due to the sum of the mirror luminescence (I_{PL}^M) and the cavity emission (I_{PL}^C):

$$I_{\mathrm{PL}}=I_{\mathrm{PL}}^M+I_{\mathrm{PL}}^C. \tag{6}$$

Though, I_{PL}^C can have a linear dependence on J_{exc}, I_{PL} has a sublinear dependence due to the mirror contribution. In fact, the absorption saturation of the mirror luminescence can be modelized in the following way:

$$I_{\mathrm{PL}}^M\propto(1-\mathscr{T})J_{\mathrm{exc}}, \tag{7}$$

where $\mathscr{T}$ is the transmission coefficient of the mirror, i.e., $(1-\mathscr{T})$ is the absorbance in the mirror layers.

$$\mathscr{T}\simeq\exp[-\chi(J_{\mathrm{exc}})d_M], \tag{8}$$

where $\chi(J_{\mathrm{exc}})$ is the excitation intensity dependent absorption coefficient of the mirror layers (with a total thickness of d_M). In a simple model[10]

$$\chi\simeq\frac{\chi^0}{(1+J_{\mathrm{exc}}/J_{\mathrm{exc}}^S)}, \tag{9}$$

and the J_{exc}^S is the saturation intensity. As J_{exc} increases, $\mathscr{T}$ increases, $(1-\mathscr{T})$ decreases and the contribution from the recombinations in the mirror spatial region decrease resulting in an $\alpha<1$. A schematic sketch of this behavior is shown in the inset of Fig. 7, where a power law fit of the resulting I_{PL} yields an $\alpha\simeq0.84$. The fact that J_{exc}^S increases for low T causes an increasing contribution of I_{PL}^M to I_{PL} at low T. This, in turn, causes a decrease in α because most of the excitons are photoexcited in the mirror region which exhibits the strong absorption saturation.

(7) No variations in ΔE_x caused by the PSM are observed because a weak exciton-photon coupling is present in PSM.

V. CONCLUSION

In this article we have deepened further our studies of the fundamental physical properties of porous silicon microcavities. PSM are almost an unique system to study the coupling of the light with a disordered system of Si nanocrystals and show important differences with respect to the physics of porous silicon and of III–V microcavities.

Both the dielectric environment and the photon-exciton coupling contribute to modify the spontaneous emission rate in PSM. In Ref. 5 the role of the dielectric environment in modifying the luminescence decay time has been demonstrated. In this article we show that it is the coupling of the confined photon mode with the singlet exciton state which reduces the singlet lifetime in the optical cavity. In contrast, the triplet exciton state whose optical transition is dipole prohibited is not affected by the cavity structure. The measurement of the temperature dependence of the lifetime allows to extract the singlet contribution to the luminescence decay time.

Unlike III–V based semiconductor microcavities, the confining mirrors play an active role in PSM. Their optical saturation affects the cavity emission properties. Hence, the mirrors do not simply confine the optical mode to the cavity layer but also act as loss regions for the cavity mode. These findings have to be taken into account in the exploitation of porous silicon microcavities for nonlinear optical applications because the theoretically predicted and experimentally observed nonlinear effects of III–V based microcavities are modified.

Being the dielectric environment critical to room temperature performances, a study of the effect of atmospheric impregnation of the PSM (i.e., ageing) is crucial and will be performed in the near future. However, we believe that the ageing does not change the overall picture which emerges from this study about the role of the dielectric environment, of the photon coupling with the singlet excitonic state and the active role of the mirrors. Finally, a theoretical modelization of PSM is needed to fully understand their optical properties.

ACKNOWLEDGMENTS

We acknowledge various enlightening discussions with L. C. Andreani. The financial support of INFM and of CNR (Grant No. 97.01383.PF48) is acknowledged. The fine Si wafers have been provided by MEMC Electronic Materials (Novara-Italy).

[1] A. G. Cullis, L. T. Canham, and P. D. J. Calcott, J. Appl. Phys. **82**, 909 (1997).
[2] G. Bjork and Y. Yamamoto, in *Spontaneous Emission and Laser Oscillation in Microcavities*, edited by H. Yokoyama and K. Ujihara (Chemical Rubber, London, 1995), p. 189.
[3] L. Pavesi, Riv. Nuovo Cimento **20**, 1 (1997).
[4] V. Pellegrini, A. Tredicucci, C. Mazzoleni, and L. Pavesi, Phys. Rev. B **52**, R14328 (1995).
[5] M. Cazzanelli and L. Pavesi, Phys. Rev. B **56**, 15264 (1997).
[6] L. Pavesi and P. Dubos, Semicond. Sci. Technol. **12**, 570 (1997).
[7] H. E. Roman and L. Pavesi, J. Phys.: Condens. Matter **8**, 5161 (1996).
[8] P. D. J. Calcott, K. J. Nash, L. T. Canham, M. J. Kane, and D. Brumhead, J. Phys.: Condens. Matter **5**, L91 (1993).
[9] E. Snoeks, A. Lagendijk, and A. Polman, Phys. Rev. Lett. **74**, 2459 (1995).
[10] C. Weisbuch and B. Vinter, *Quantum Semiconductor Structures: Fundamentals and Applications* (Academic, Boston, 1991), p. 96.